

Following Plant Metabolism *in Vivo* and in Extracts with Heteronuclear Two-Dimensional Nuclear Magnetic Resonance Spectroscopy¹

Yair Shachar-Hill,* Philip E. Pfeffer,*² and Markus W. Germann†

*United States Department of Agriculture, Agricultural Research Service, Eastern Regional Research Center, 600 E. Mermaid Lane, Wyndmoor, Pennsylvania 19038; and †Kimmel Cancer Institute, Thomas Jefferson University, Philadelphia, Pennsylvania 19107

Received June 5, 1996

Limits of sensitivity and spectral resolution currently restrict the application of nuclear magnetic resonance (NMR) spectroscopy in plant metabolism. This study shows that these limits can be substantially expanded through the application of heteronuclear single- and multiple-quantum two-dimensional (2D) spectroscopic methods using pulsed field gradients both *in vivo* and in extracts. The course of metabolism in approximately 0.2 g of maize (*Zea mays* L.) root tips labeled with [1-¹³C]glucose was followed with 1 min time resolution using heteronuclear multiple quantum coherence (HMQC) ¹³C-¹H spectroscopy *in vivo*. The timing of alanine, lactate, and ethanol synthesis was followed during the transition from normal to hypoxic conditions. In extracts of labeled maize root tips, ¹³C-¹H heteronuclear single quantum coherence and heteronuclear multiple quantum coherence (HMBC) spectra acquired in 2–3 h allowed the detection and assignment of resonances that are not seen in one-dimensional (1D) ¹³C NMR spectra of the same samples taken in 12 h. In root tips labeled with ¹⁵NH₄⁺, ¹⁵N-¹H HMQC spectra *in vivo* showed labeling in the amide of glutamine. In extracts, ¹⁵N labeling in amines and amides was detected using ¹⁵N-¹H HMBC spectra that is not seen in 1D ¹⁵N spectra of the same sample.

Nuclear magnetic resonance (NMR)³ spectroscopy *in vivo* together with the use of ¹³C- and ¹⁵N-labeled sub-

¹ Mention of brand or firm name does not constitute an endorsement by the U.S. Department of Agriculture over others of a similar nature not mentioned.

² To whom correspondence should be addressed. Fax: +1 (215) 233-6581.

³ Abbreviations used: 1D, one dimensional; 2D, two dimensional; HMBC, heteronuclear multiple bond coherence; HMQC, hetero-

strates has proved, in the past 20 years, to be a powerful method for studying metabolism in living systems. In plant physiology much unique information has been obtained addressing a range of metabolic problems (reviewed in 1–3). The limits of the temporal and biochemical information obtained in these studies has hitherto been set by the sensitivity with which signals can be obtained and by the separation of signals (spectroscopic resolution) obtainable in directly detected, 1D spectra. Sensitivity of detection has generally limited the time resolution available in ¹³C spectroscopy of single samples of plant tissues to 10 min or more and is substantially worse for ¹⁵N. The sample sizes used for this time resolution are several grams (e.g., several hundred to several thousand root tips per sample) and this in turn has prevented the application of *in vivo* NMR to many problems in plant biochemistry where more limited quantities of tissue or lower levels of metabolites are available. Fan and co-workers (4–6) have demonstrated the much greater sensitivity of ¹H spectroscopy for detecting plant metabolites as well as the improved spectroscopic resolution available in homonuclear ¹H two-dimensional (2D) spectroscopy. This approach allows measurement of metabolite levels but does not give the information on metabolic fluxes that isotopic labeling methods yield. In order to follow isotopic labeling using the sensitivity of ¹H spectroscopy, methods of “indirect detection” have been employed in animal studies to follow the metabolism of ¹³C-labeled compounds (reviewed in 7). (In indirectly detected spectra, ¹H signals are selectively observed from hydrogens coupled to ¹³C or ¹⁵N atoms.) Indirect detection has

nuclear multiple quantum coherence; HSQC, heteronuclear single quantum coherence; Mes, 2-[N-Morpholino]-ethane-sulfonic acid; NMR, nuclear magnetic resonance; NOE, nuclear Overhauser effect; S/N, signal-to-noise ratio; T₂, transverse relaxation time.

recently also been used to follow ^{15}N label in supernatants from mammalian cells (8) and in plant extracts (9). Methods that have the advantages of ^1H sensitivity and of multidimensional spectroscopic resolution have been developed for structure determination (10–12); and recently these have been shown to have potential for following ^{13}C labeling in animal metabolic studies (13). Plant studies present different technical challenges for *in vivo* NMR because metabolic fluxes per volume of tissue are lower than in animals or microorganisms and because perfusion needed to maintain tissues during NMR experiments makes effective suppression of the dominant water signal challenging. Plant tissue samples can be small and this makes *in vivo* spectroscopy at high field feasible; this in turn presents challenges associated with high frequencies and larger bandwidths. In this study we have sought to explore the potential of heteronuclear multiple quantum coherence spectroscopic methods for following metabolism in roots under normal and hypoxic conditions. Maize root tips were used since this is the most widely used tissue in plant NMR spectroscopic studies (1–3) and therefore allows the most meaningful comparisons with existing methods and metabolic findings.

METHODS

NMR Spectroscopy

NMR experiments were recorded on a Bruker AMX600 NMR spectrometer equipped with a S-17 Acqstar gradient amplifier and a digital gradient interface. The gradient probehead was a Bruker 5-mm triple resonance (^1H , ^{13}C , ^{15}N) inverse probehead with a self-shielded Z gradient coil (6 G/cm A). The pulse sequence that was used for the *in vivo* gradient-assisted HMQC spectra (see Ref. 12) is shown in Fig. 1. Presaturation of the water for between 300 ms and 1 s was used to suppress this signal in addition to its exclusion based on coherence pathway selection (12). This combination gave very efficient suppression of water signals in perfused tissue samples. For the ^{13}C - ^1H HMQC and HSQC (10–12) experiments, Garp ^{13}C decoupling was applied during the acquisition period. All gradients were applied as 128 point sine bell shapes with a duration of 1.5 ms. The gradient recovery delay was set to 20 μs for experiments on extracts and 100 μs for the *in vivo* experiments. For HMQC (10) and HMBC (11) experiments, gradients were applied for coherence pathway selection. The gradient ratio for the ^{13}C - ^1H HMQC *in vivo* was 36:36:18.08 G/cm while for the ^{15}N - ^1H HMQC *in vivo* spectra the gradient ratio was 24:24:4.86 G/cm. In ^{13}C - ^1H HMBC (11) extract experiments a ratio of 6:6:3.02 G/cm was used and the evolution delay for the long range couplings was set to 50 ms; a low-pass filter, set to 140 or 100 Hz was used to suppress the one-bond heteronuclear couplings. Phase-

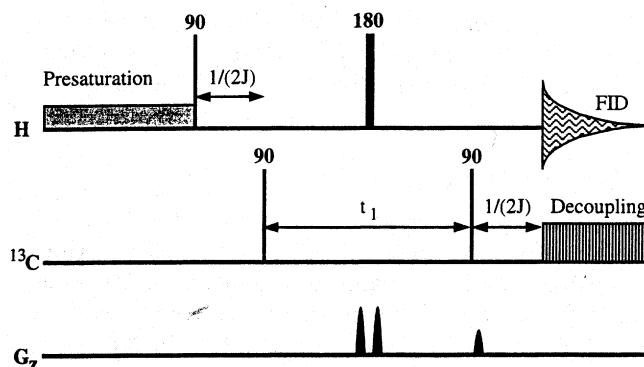


FIG. 1. The pulse sequence used for recording ^{13}C - ^1H HMQC magnitude mode spectra of perfused root tips. The ^1H , ^{13}C , and gradient pulses are depicted on separate lines. This sequence was found to be more robust for *in vivo* spectroscopy than other indirectly detection 2D pulse sequences that employ more than this minimum number of pulses. Weak presaturation at the water frequency was applied during the relaxation delay in order to further suppress the water signal. With this scheme, receiver gains of 16K–32K were typically achieved during perfusion.

sensitive HSQC (12) data were recorded using gradients for coherence pathway rejection, giving full sensitivity spectra. In this case gradients were applied at 12, -7.2 , and -2.4 G/cm. One-dimensional ^{13}C and ^{15}N spectra were acquired on the same spectrometer for extracts and also on a Unity Plus Varian 400 instrument. Proton decoupling was used throughout for maximal nuclear Overhauser effect (NOE) enhancement. *In vivo* 1D ^{13}C spectra (see below) were acquired using the Unity Plus Varian 400 instrument in a 10-mm broadband probe with 90° pulses and recycle times of 2 s. Total acquisition times were 22 min. 2D NMR data were processed using XWINNMR 1.1 software running on a Silicon Graphics INDY workstation. Raw data were zero-filled to 512 or 1K points in the acquisition dimension and were filtered using a shifted sine bell function in both dimensions before Fourier transformation. No base-plane correction was applied.

Labeling Experiments

Corn (*Zea mays* L. Cultivar W 7551) seeds were germinated and grown for 3 days in the dark at 30°C as previously described (14). Root tips (5 mm long) were cut into an oxygenated solution containing 10 mM glucose, 0.1 mM Ca^{2+} (as chloride or sulfate) and buffered to pH 6.0 with 10 mM Mes.

For extract preparation 2–4 g of root tips were transferred into 250 ml of solution containing 10 mM ^{13}C -labeled glucose, 5 mM $^{15}\text{NH}_4\text{Cl}$ with 0.1 mM Ca^{2+} (as chloride or sulfate) and buffered to pH 6.0 with 10 mM Mes and were oxygenated for 6 h. The root tips were then removed, rinsed with water, and extracted in 100 ml of boiling 80% ethanol: 20% water for 10 min. The

extracts were then filtered and the ethanol was removed by rotary evaporation, the samples were then lyophilized. Extracts were dissolved in D₂O for spectroscopic analysis.

In Vivo Spectroscopy

Root tips were cut as above and 50–100 (about 0.2 g) were transferred to a 5-mm NMR tube in which they were perfused with the same oxygenated buffer solution used for extracts. The perfusion medium (total volume 300 ml) was circulated through the sample from a reservoir using a peristaltic pump, perfusion rates were between 5 and 15 ml/min. For *in vivo* time courses ($n = 4$) tips were incubated for 3–6 h before the onset of hypoxia. Hypoxia was induced by switching the perfusion from buffer solution bubbled with oxygen to buffer bubbled with nitrogen to remove and exclude dissolved oxygen. For 1D *in vivo* ¹³C spectroscopy approximately 500 root tips, 5 mm long (about 2 g), were placed in a 10-mm NMR tube and perfused as for the smaller samples but with higher rates of perfusion (20–30 ml/min).

RESULTS AND DISCUSSION

Figure 2 shows two of a series of *in vivo* ¹H–¹³C HMQC spectra (see Methods) taken of maize root tips perfused with 10 mM [1-¹³C]glucose. In such spectra proton signals appear only from those ¹H atoms directly coupled to ¹³C carbon atoms (10). The resonances are dispersed along the horizontal axis by the ¹H chemical shift of the corresponding 1D proton spectrum and along the vertical axis by the ¹³C chemical shift of the carbon atom to which the proton is coupled.

Figure 2A was acquired after 3 h of labeling during perfusion with oxygenated buffer. After the spectrum of Fig. 2A was acquired, the root tips were perfused for an additional 1.5 h and then made hypoxic in the same perfusion medium. Figure 2B was acquired after 1 h of hypoxia. The HMQC resonances shown in Fig. 2 were assigned as arising from different metabolites by comparison with HSQC and HMBC spectra of extracts (see below) and by comparison with known chemical shifts of ¹H and ¹³C metabolite signals (3, 5, 15). The quality of these spectra (acquired in 20 min using approximately 70 maize root tips) shows the feasibility of applying gradient-assisted HMQC at high field *in vivo* and with perfusion to the detection of ¹³C in metabolites. Suppression of the water signal at high field *in vivo* using presaturation and pulsed-field gradient methods is extremely effective despite continuous perfusion. The sensitivity of this method was compared to ¹³C 1D spectroscopy by reference to studies in the literature (1, 3, 17, 18 and references therein) and by acquiring a time course of 1D ¹³C spectra from a sample of 500 root tips grown and perfused under the same

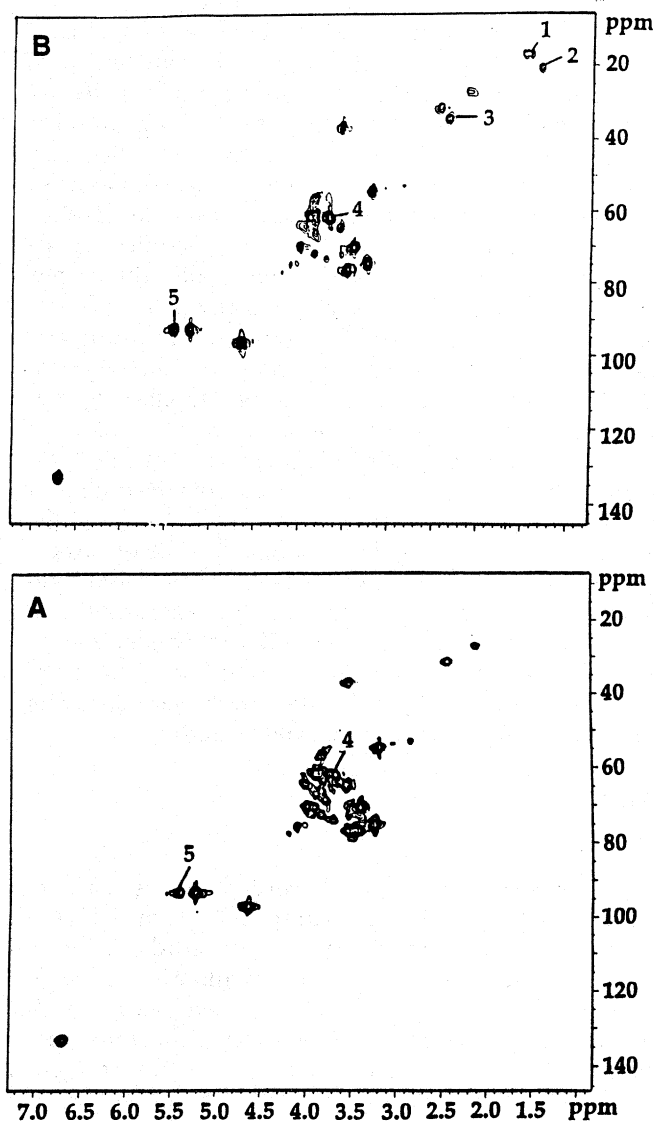


FIG. 2. Two ¹³C–¹H heteronuclear multiple quantum coherence spectra of perfused maize root tips. Approximately 0.2 g of 5-mm root tips were perfused with buffered nutrient solution in a 5-mm NMR tube in the magnet of the spectrometer (see Methods). The sample was perfused with oxygenated buffer containing 10 mM [1-¹³C]glucose for 3 h before the acquisition of spectrum A was begun. Thereafter the sample was perfused for an additional 1.5 h and the sample was made hypoxic; acquisition of the spectrum B was begun after 1 h of hypoxia. Attention is drawn to certain of the ¹³C-labeled resonances that change in intensity between the spectra: 1, methyl group of alanine; 2, methyl group of lactate; 3, C3 of glutamate and of glutamine; 4, C1 of the fructose moiety of sucrose; 5, C1 of the glucose moiety of sucrose. Each spectrum took 20 min to acquire.

conditions as those of Fig. 2 (with the exception that perfusion was in a 10-mm probe of a 400-MHz instrument—see Methods). Spectra (not shown) of this much larger sample (volume of tissue in the sensitive volume was over 8 times as large in the 10-mm probe) taken in 22 min had signal-to-noise ratios (S/N) comparable

to 1D spectra in the literature—that is at least 10 times lower than the S/N in 1D projections of the spectra of Fig. 2 (see Fig. 3B below). This is consistent with the greater sensitivity of indirect detection (reviewed in 7). The proton linewidths in this 5-mm sample at 600 MHz are comparable with *in vivo* linewidths for maize at lower fields (5). The resolution in the carbon dimension is limited by the number of increments in this dimension and by inhomogeneity; for many resonances it is worse than the resolution obtained in 1D ^{13}C spectra of larger volumes of maize root tips *in vivo* (1D spectra from 400 MHz instrument, not shown). The added resolution due to the proton dimension offsets this somewhat so that for example the number of resonances partially or fully resolved between 55 and 85 ppm in the ^{13}C dimension (where most carbohydrate carbons resonate) were very similar in the 1D ^{13}C *in vivo* spectrum (not shown) and in the *in vivo* HMQC spectra. In particular cases there are differences in resolution so that the C1 resonance of sucrose which is never resolved from the C1 resonance of α -glucose in 1D ^{13}C spectra *in vivo* is fully resolved in Fig. 2 (labeled 5). On the other hand glutamate and glutamine resonances between 25 and 40 ppm are better resolved in 1D carbon spectra. Visual comparison of Figs. 2A and 2B shows that labeling in the C3 carbons of alanine and lactate (marked 1 and 2) and in the C3's of glutamate and glutamine (labeled 3) have changed substantially during the experiment. This is consistent with previous studies (1, 16). By comparing the intensities of corresponding signals in Figs. 2A and 2B (in 1D projections or by volume integration of 2D peaks) it was seen that the C1 and C1' carbons of sucrose (labeled 4 and 5) had substantially decreased after hypoxia.

The early metabolic changes that occur upon depriving plant cells of oxygen have been extensively studied by NMR and other methods (reviewed in 18 and 19). The timing of the onset of fermentation under hypoxia and the relative rates of production of alanine, lactate, and ethanol are important in testing models of how primary metabolism and pH interact. This in turn is important in understanding how plant roots survive flooding and the resultant oxygen deprivation. Because of extensive previous work and the rapidity of changes involved, the onset of hypoxia in maize root tips has appeal for testing the application of HMQC to plant metabolism *in vivo*.

Although the spectra of Fig. 2 were acquired in 20 min, sufficient signal-to-noise to follow labels may be obtained in much less time by using projections and volume integration of individual peaks in HMQC spectra. Figure 3A shows a stacked plot representation of the methyl region of an *in vivo* ^{13}C - ^1H HMQC spectrum acquired in 8 min of maize root tips during hypoxia in the presence of ammonia. This representation shows the separation obtained in these resonances by

this method. By contrast, the ethanol resonance is incompletely resolved (when detected) in 1D ^{13}C spectra *in vivo* (16, 20). The high S/N and flat baselines allow monitoring of metabolite signals with greater confidence than is possible in 1D ^{13}C spectra. Indeed it was possible, by reducing the number of scans per increment to 1 and restricting the number of increments, to acquire *in vivo* HMQC spectra in 63 s. Figure 3B shows projections in both the proton and carbon dimensions of the methyl region of such an *in vivo* HMQC spectrum taken in a minute. The S/N obtained in spectra like Fig. 3B is superior to 1D ^{13}C spectra taken from much larger samples in significantly longer times. Figure 3C shows the time course of changes in the signals of the methyl groups of alanine, lactate, and ethanol upon switching the perfusing medium from oxygenated to hypoxic conditions (see Methods). Each point in Fig. 3C represents the height of the corresponding peak in spectra such as those of Fig. 3B. The samples for such time courses were exposed to $[1-^{13}\text{C}]$ glucose for several hours before Time 0 of Fig. 3C because it has been shown (21) that labeling of metabolites reaches steady state under these conditions. This means that the changes seen in peak height represent changes in the levels of these metabolites. Thus it may be seen that upon exposure to hypoxia in the presence of ammonia, alanine is produced with little or no lag, while detectable levels of lactate only appear some 4 min later. Several more minutes then elapse before ethanol can be detected, though it is then synthesized faster than lactate. The lag following the removal of oxygen before lactate synthesis begins has not been previously reported. For example Saint-Ges and co-workers (22) used extraction of maize root tip samples (50 tips taken every 5 min) and enzymatic assay to follow lactate production in hypoxia and reported that "lactate accumulated steadily during the first 30 minutes of hypoxia." Xia and Saglio (23) also used *in vitro* assays to follow lactate and ethanol production in maize root tips with samples taken every 5 min or more after the onset of hypoxia. These authors reported lactate production "right after the transition to hypoxia." Recently, a lag in lactate production of "a couple of minutes" has been found by Roberts and Xia (in Ref. 3) in maize root tips by adding *in vivo* 1D ^{13}C spectra from six replicate experiments, each apparently containing several hundred to 2000 root tips which had been labeled for 16 h with $[1-^{13}\text{C}]$ glucose to maximize ^{13}C enrichment. The 4-min lag shown here is not consistent with the early data (20) suggesting that lactate production causes the rapid acidification of the cytoplasm. Although this conclusion has been questioned (see 18, 19), the present data provide rather direct evidence on this question. Concerning ethanol production, it has been shown by enzymatic assay that there is a 10-min lag, after the onset of hypoxia in perfused maize root tips, before

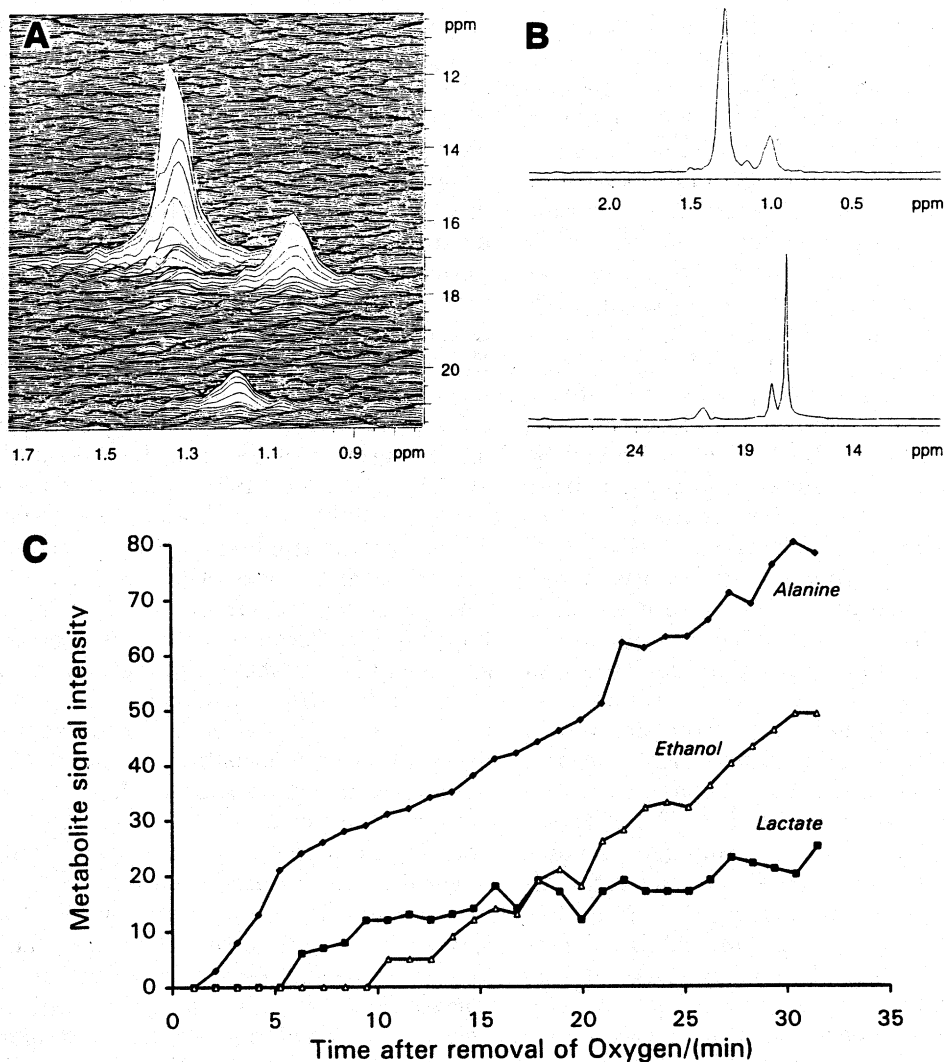


FIG. 3. Following the transition from oxygenated to hypoxic conditions in maize root tips using ^{13}C - ^1H heteronuclear multiple quantum coherence spectroscopy. (A) Methyl region of an *in vivo* spectrum acquired from perfused maize root tips (see Methods and legend to Fig. 2) in 8 min beginning after half an hour of hypoxia. Peaks arise from ^{13}C labeling in the CH_3 groups of: I, Alanine; II, Ethanol; III, Lactate. (B) Two partial projection (top, projection onto the proton dimension; bottom, projection onto the carbon dimension) from the methyl region of an *in vivo* HMQC spectrum acquired in 63 s. (C) Time course of the production of alanine, ethanol, and lactate derived from *in vivo* HMQC spectra.

ethanol appears in the perfusate (20) or in samples of tissue and perfusate together (23). Note that the levels of ethanol, lactate, alanine, and other metabolites produced by the tissue and potentially secreted into the perfusing medium are too low to be detected in these spectra. This is primarily because of the small amount of tissue (approximately 0.1 ml of cells) relative to the volume of the perfusing medium (300 ml). Therefore the time course of Fig. 3C reflects ethanol in the sample rather than in the medium and shows the same lag of 10 min before ethanol is detected as was seen in previous studies where ethanol in the medium was analyzed. Thus the lag in the appearance of ethanol in the

effluent in previous studies is due to a lag before ethanol synthesis increases. The ability to monitor intracellular metabolite levels on this time scale allows one to examine metabolic models in detail. Thus ethanol production is stimulated at a time after cytoplasmic pH has fallen significantly while alanine synthesis is stimulated immediately as oxygen levels fall; lactate production begins at an intermediate time. In addition, the use of gradients in the pulse sequence causes marked attenuation of signals from compounds in the perfusate. This is because the gradient pulses impose different field strengths at different points in the sample, so that molecules which move significantly during

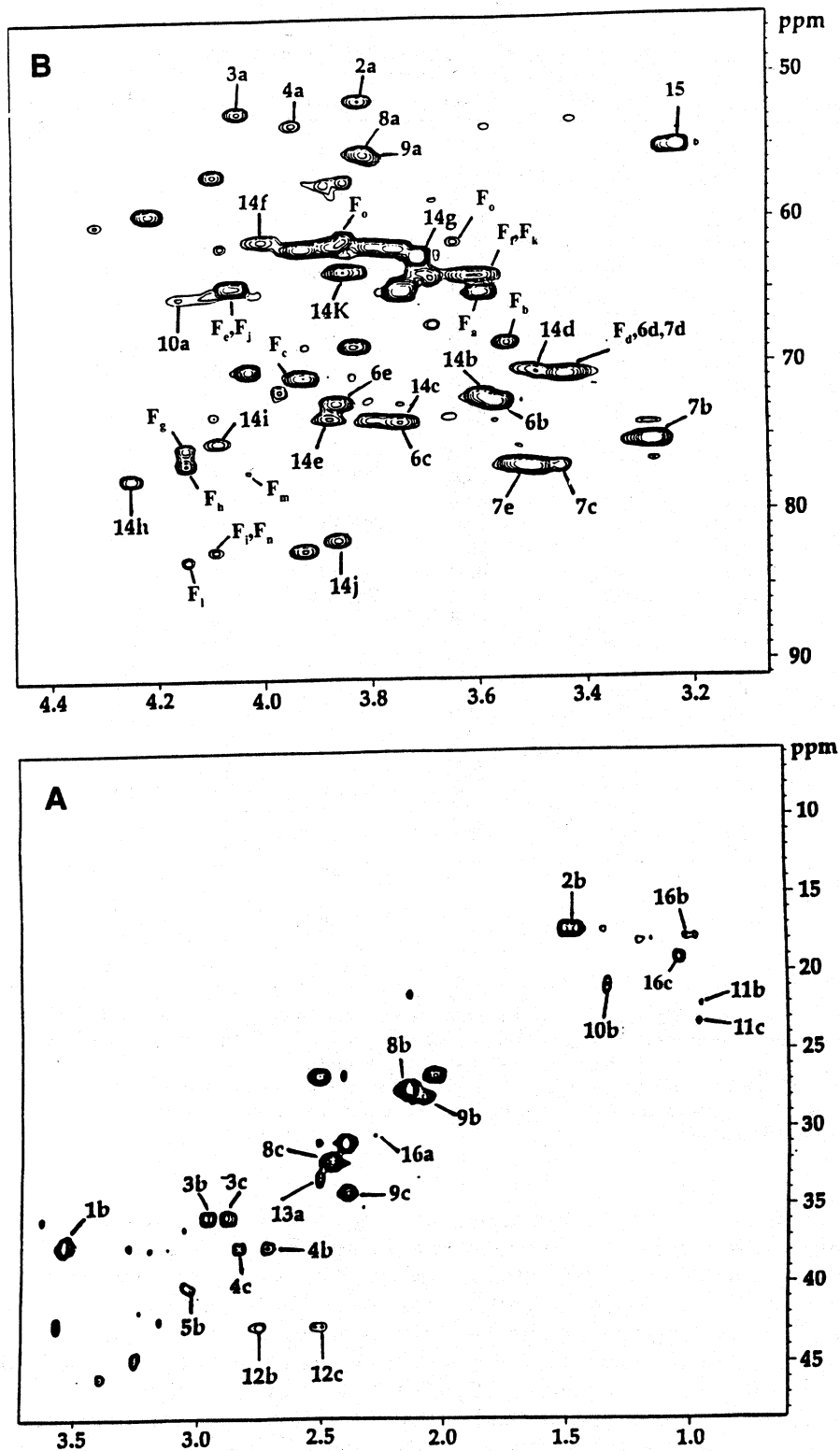


FIG. 4. Identifying ^1H - ^{13}C signals from a crude extract of maize root tips. Two regions from a ^{13}C - ^1H heteronuclear single quantum coherence spectrum of an ethanol/water extract of approximately 2 g of maize root tips that had been labeled by incubation with [1,2- ^{13}C]glucose for 6 h in the presence of 5 mM ammonium under oxygenated conditions. The labeling of resonances refers to Table 1. (A) Up-field region. (B) Low-field region. The spectrum was acquired in 2.5 h.

TABLE 1'
Assignments of Resonances in HSQC of *Zea mays* Extract

Compound	Label	Portion	¹ H shift	¹³ C shift	Compound	Label	Portion	¹ H shift	¹³ C shift
t-Aconitate	1a	αCH ₂	6.73	133	Glucose β	7a	C1	4.64	97.0
	1b	γCH ₂	3.5	37.5		7b	C2	3.24	75.0
Alanine	2a	αCH	3.82	51.7		7c	C3	3.47	76.7
	2b ^b	βCH ₃	1.48	17.0		7d	C4	3.64	70.5
Asparagine	3a	αCH	4.01	52.6		7e	C5	3.49	76.7
	3b	β'CH	2.88	35.9	Glutamine	8a	αCH	3.8	55.3
	3c	βCH	2.95	35.9		8b	βCH ₂	2.13	27.4
Aspartate	4a	αCH	3.94	52.9	8c	γCH ₂	2.45	32.0	
	4b	βCH	2.71	37.9	Glutamate	9a	αCH	3.86	55.4
	4c	β'CH	2.85	37.9		9b	βCH ₂	2.06	28.0
Fructose-β-pyranose	Fa	C1	3.59	64.8	9c	γCH ₂	2.38	34.6	
	Fb	C3	3.55	68.9	Lactate	10a	βCH ₂	4.13	65.0
	Fc	C4	3.42	70.5		10b	CH ₃	1.32	20.5
	Fd	C5	3.93	70.08	Leucine	11b	δCH ₃	0.93	22.0
	Fe	C6	4.06	64.4		11c	δ'CH ₃	0.95	23.0
Fructose-β-furanose	Ff	C1	3.60	63.6	Malate	12b	CH	2.75	43.0
	Fg	C3	4.15	76.4		12c	'CH	2.48	43.0
	Fh	C4	4.15	75.5	Succinate	13a	CH ₂	2.5	33.0
	Fi	C5	4.09	82.0		Sucrose	14a	G1	5.41
	Fj	C6	4.06	64.4	14b		G2	3.59	71.0
	Fructose-α-furanose	Fk	C1	3.68	63.8		14c	G3	3.78
Fl		C3	4.13	82.9	14d		G4	3.46	70.5
Fm		C4	4.02	77.0	14e	G5	3.56	73.1	
Fn		C5	4.11	82.2	14f	G6	3.18	61.5	
Fo		C6	3.64, 3.86	61.9	14g	F1	3.68	62.2	
GABA		5a	γCH ₂	3.0	40.5	14h	F3	4.23	77.3
Glucose α	6a	C1	5.22	93.0	14i	F4	4.09	74.8	
	6b	C2	3.54	72.3	14j	F5	3.85	82.19 ^c	
	6c	C3	3.71	73.5	14k	F6	3.84	63.2	
	6d	C4	3.40	70.4	Choline	15a	N(CH ₃) ₃	3.24	55
	6e	C5	3.87	72.4		15b	αCH ₂	3.85	69.0
					Valine	16a	CH ₂	2.25	30.5
						16b	CH ₃	0.9	17.8
						16c	CH ₃	1.0	19.0

^a The pH of this extract was close to 5.5. While both natural abundance and labeled signals are seen in HSQC spectra like those of Fig. 4, not all the resonances are observed from each compound because labeling from [1,2-¹³C]glucose does not label all positions and signal intensity from natural abundance peaks is insufficient for less abundant compounds.

^b It is not trivial to ¹³C decouple across the whole spectrum at high field in conductive samples and we observed residual couplings in some of the methyl resonances. This coupling was removed at higher decoupling powers (not shown).

^c To which other signals were referenced.

the pulse sequence experience different field strengths during the sequence; such molecules do not give rise to a gradient echo so that no signal is observed from them. Glucose was the only metabolite present in the perfusate at significant levels in these experiments and we observed that its signals more than doubled (relative to other signals) when the perfusion was turned off (not shown). Since the glucose signals come from both intracellular and extracellular glucose, this shows an attenuation of extracellular signals relative to intracellular ones by a factor of at least 2.

We used HSQC and HMBC spectroscopy of maize root extracts in order to confirm assignments in *in vivo* spectra (Figs. 2 and 3) and in order to explore the utility

of using 2D ¹H-detected heteronuclear spectroscopy for detecting labeling in plant metabolites in crude extracts. Figure 4 shows two parts of a ¹H-¹³C HSQC spectrum of an extract of maize root tips that had been incubated for 6 h in [1,2-¹³C]glucose before extraction. By comparison with the *in vivo* HMQC spectrum of Fig. 2 the HSQC spectrum of Fig. 4 shows the same resonances but with greater resolution. Resonance labels refer to Table 1 that lists the positions of the compounds whose signals were assigned in HSQC and HMBC ¹³C-¹H spectra. The spectrum of Fig. 4 was acquired in 2.5 h. A number of points can be made concerning the utility of this method:

The dispersion in two dimensions allows greater con-

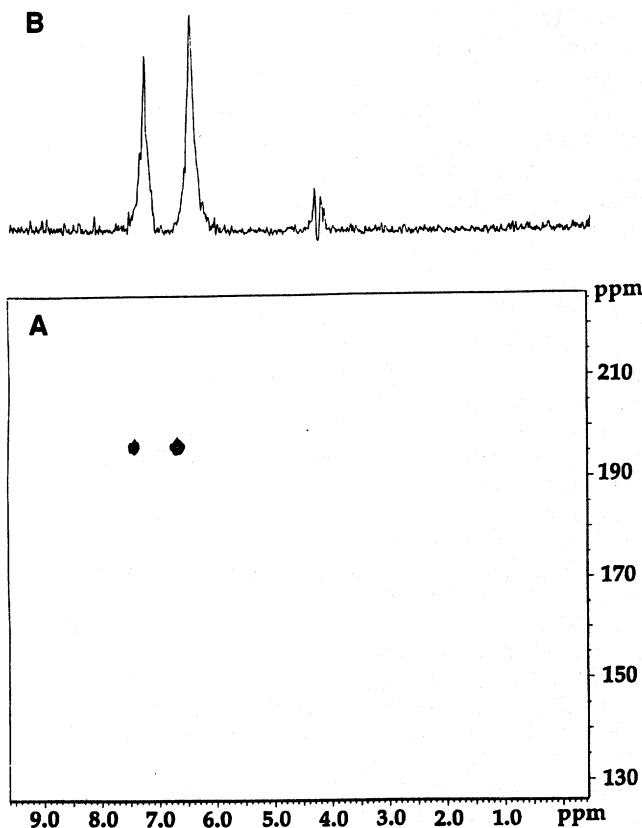


FIG. 5. Detecting ^{15}N labeling in the amide of glutamine in maize root tips using ^{15}N - ^1H heteronuclear multiple quantum coherence spectroscopy. The sample was the same as that used to obtain the spectra of Fig. 2 and was obtained in 10 min after approximately 4 h of exposure to 5 mM ^{15}N -labeled ammonium under oxygenated conditions. (A) Part of the HMQC spectrum; (B) a projection of the full spectrum onto the ^1H dimension. In both A and B the peaks arise from the two nonequivalent amide protons of glutamine that has become ^{15}N -labeled in the amide position. In the middle of B there is a small residual water signal.

confidence in making assignments than is possible in one-dimensional spectra. In assigning 1D spectra, additional information from mass spectrometry and from spectra acquired at varying pH and/or after the addition of known compounds is routinely needed (1-6). The present method greatly reduces the need for such additional information (15) for assigning spectra. This is because while there is often more than one possible compound that could account for a resonance with a particular carbon or proton chemical shift, many fewer resonances share the same carbon *and* proton shifts. This makes assignment by comparison with spectroscopic tables (3, 15) much more straightforward. The dispersion in two dimensions separates resonances that overlap in 1D spectra (especially in ^1H spectra), making separate quantitation possible. However, resolution in the ^{13}C dimension in HSQC and HMQC spectra is inferior to that obtained in 1D ^{13}C spectra so that

there are some cases where resonances can be resolved in the 1D ^{13}C spectrum that overlap in Fig. 4. The sensitivity with which ^{13}C -containing compounds (both labeled and natural abundance) are detected in Fig. 4 is much greater than in 1D ^{13}C spectroscopy. For example, Fig. 4 contains signals from ^{13}C in leucine, valine, and the furanose forms of fructose that we did not observe in 1D ^{13}C extract spectra and which have not previously been reported in such spectra of plant extracts despite much longer acquisition times (typically 12-24 h). We note that there is potential for even better resolution in the ^{13}C dimension by using heteronuclear correlation spectra (HETCORR, 3, 15) which give similar spectra to HSQC but which are detected in ^{13}C . However, HETCORR spectra require long acquisition times and are insensitive to metabolites present at low levels because the signal is acquired from ^{13}C not ^1H nuclei. The increased dispersion, information content, and sensitivity of HSQC relative to 1D spectra allow the detection and separation of a significant number of resonances that remain at present unassigned because to our knowledge they have not previously been seen in spectra of plant or animal extracts. Work is underway to assign these. ^1H - ^{13}C HMBC spectra give connectivities within a molecule because correlation peaks appear which have the carbon chemical shift of any given carbon and the proton shifts of hydrogens in the same molecule that are more than one chemical bond away (11). Thus assignments from HSQC spectra can be confirmed and peaks appear from carbons that do not give HSQC peaks because of not having directly bonded protons. To explore the potential of this method, HMBC spectra were taken of the same extracts from which HSQC spectra were acquired (data not shown). We were able to confirm assignments of some of the metabolites in Table 1 and to detect labeling and natural abundance signals from carboxyl carbons of glutamate, glutamine, alanine, and *trans*-aconitate and from the double-bonded carbons of *trans*-aconitate. This method provides extra information for assignments and gives greater sensitivity on carbonyl and other carbons that are not directly bonded to hydrogen atoms. Such carbons give poor S/N in ^{13}C spectra because of long relaxation times and lack of NOE in directly detected 1D ^{13}C spectra. However, HMBC was found not to be useful *in vivo* because the faster transverse relaxation (shorter T_2) of metabolites *in vivo* very greatly reduced the signal strength. We note that for comparable acquisition times in extract spectra (2-3 h) the S/N in some HMBC peaks is lower than in HSQC (for example, ^{13}C in malate and citrate that gave rise to signals in HSQC spectra was not detected in an HMBC spectrum acquired in comparable acquisition time). This, in part, is because the relative intensity of different peaks is rather sensitive to spectroscopic mixing times so that quantitation (or even assessing

relative labeling in different positions within a molecule) from HMBC spectra requires knowledge of coupling constants and relaxation times for the protons and carbons involved.

The application of 2D multiple quantum methods to following ^{15}N labeling in plants was also assessed. In extracts, ^{15}N - ^1H HMQC and HMBC allow the detection and resolution of labeled amino acids with greater sensitivity in 1 h than was possible in 1D ^{15}N spectra in 48 h. (data not shown). This parallels findings by Street *et al.* (8) in supernatants from mammalian cell cultures. HMBC in particular allows resolution of signals from labeled amino acids whose ^{15}N primary amine signals are poorly resolved. The sensitivity enhancement due to indirect detection of ^{15}N is more marked than that of ^{13}C . This is shown in Fig. 5 which contains the HMQC spectrum and a projection of the same taken in 10 min of the same sample of maize root tips from which the spectra of Fig. 2 were acquired. The two signals are both due to ^{15}N -labeled glutamine after 3 h of labeling with 5 mM ^{15}N -labeled ammonium. The S/N in the projection of shown in Fig. 5B is superior to S/N in 1D ^{15}N spectra of a variety of plant cell and root tissue samples (reviewed in 1, 3). This is despite the fact that the sample size here was 10–40 times smaller than in other studies (1, 3) and the acquisition time was 3–12 times shorter. Unfortunately due to rapid exchange of protons at physiological pH the HMQC signals from primary amine groups cannot be detected *in vivo* by this approach, whereas it can be seen in 1D ^{15}N spectra. HMBC can be used to overcome this in extracts by detecting proton signals from ^1H atoms coupled to the ^{15}N -labeled amine groups through several bonds. However, the smaller couplings involved require longer evolution times that are incompatible with *in vivo* T_2 relaxation rates. A 1D HMQC sequence has been used to detect glutamine in brain and liver tissue (24). Derivatized amino acids from plant extracts have been used with indirect detection of ^{15}N labeling to study amino acid and protein turnover (9). Consistent with these studies, we found significant gains in both sensitivity (at least 10-fold reductions in acquisition times) and in resolution relative to directly observed 1D ^{15}N spectra by using gradient-assisted ^{15}N - ^1H HMBC (not shown). We found that the indirect detection methods for both ^{15}N and ^{13}C (especially at 600 MHz) are more sensitive to the presence of salt in extracts than is direct detection. Thus ethanol/water extraction is preferable to extraction procedures, such as those using perchloric acid that dissolve more salts. For ^{15}N *in vivo* work, heteronuclear multiple quantum methods seem only applicable to amide and other nitrogens whose hydrogens exchange slowly at near-neutral pH, though for this purpose significant sensitivity gains are also made.

We conclude that for studying metabolism, heteronuclear multiple quantum spectroscopy at high field confers advantages compared to 1D NMR spectroscopy both *in vivo* and in extracts. Those advantages include greater information for assignment of resonances, greater sensitivity, and therefore use of smaller samples and greater time-resolution for *in vivo* studies than has hitherto been possible.

REFERENCES

1. Ratcliffe, R. G. (1994) *Adv. Bot. Res.* **20**, 43–123.
2. Roberts, J. K. M. (1987) in *The Biochemistry of Plants* (Davies, D. D., Ed.), Vol. 13, pp. 181–227, Academic Press, San Diego.
3. Shachar-Hill, Y., and Pfeffer, P. E. (Eds.) (1996) *NMR in Plant Biology*, pp. 1–260, American Society of Plant Physiologists, Rockville, MD.
4. Fan, T. W. M., Higashi, R. M., Lane, A. N., and Jardetzky, O. (1986) *Biochim. Biophys. Acta* **882**, 154–167.
5. Fan, T. W. M., Higashi, R. M., and Lane, A. N. (1986) *Arch. Biochem. Biophys.* **251**, 674–687.
6. Fan, T. W. M., Higashi, R. M., and Lane, A. N. (1988) *Arch. Biochem. Biophys.* **266**, 592–606.
7. Morris, P. G., Bader-Goffer, R. S., Prior, M. J. W., and Bachelard, H. S. (1994) in *Magnetic Resonance Scanning and Epilepsy* (Shorvon, S. D., *et al.*, Eds.), pp. 235–240, Plenum Press, New York.
8. Street, J. C., Delort, A. M., Braddock, P. S. H., and Brindle, K. M. (1993) *Biochem. J.* **291**, 485–492.
9. Ma, Y. Z., and Gent, M. P. N. (1995) *Plant Physiol.* **108**, 30.
10. Hurd, R. E., and John, B. K. (1991) *J. Magn. Reson.* **91**, 648–653.
11. Willker, W., Leibfritz, D., Kerssebaum, R., and Bermel, W. (1993) *Magn. Reson. Chem.* **31**, 287–292.
12. Wider, G., and Wuthrich, K. (1993) *J. Magn. Reson. Ser. B* **102**, 239–241.
13. Van Zijl, P. C. M., Chesnick, A. S., Despres, D., Moonen, C. T. W., Ruizcabello, J., and Vangelder, P. (1993) *Magn. Reson. Med.* **30**, 544–551.
14. Shachar-Hill, Y., Pfeffer, P. E., and Ratcliffe, R. G. (1996) *J. Magn. Reson. Ser. B* **111**, 9–14.
15. Fan, T. W. M. (1996) *Prog. NMR Spectrosc.* **28**, 161–219.
16. Roberts, J. K. M., Hooks, M. A., Miaullis, A. P., Edwards, S., and Webster, C. (1992) *Plant Physiol.* **98**, 480–487.
17. Xia, J. H., and Roberts, J. K. M. (1994) *Plant Physiol.* **105**, 651–657.
18. Ratcliffe, R. G. (1997) *Ann. Bot.*, in press.
19. Ricard, B., Couee, I., Raymond, P., Saglio, P. H., Saint-Ges, V., and Pradet, A. (1994) *Plant Physiol. Biochem.* **32**, 1–10.
20. Roberts, J. K. M., Callis, J., Wemmer, D., Walbot, V., and Jardetzky, O. (1984) *Proc. Natl. Acad. Sci. USA* **81**, 3379–3383.
21. Dieuaide-Noubhani, M., Raffard, G., Canion, P., Pradet, A., and Raymond, P. (1995) *J. Biol. Chem.* **270**, 13147–13159.
22. Saint-Ges, V., Roby, C., Bligny, R., Pradet, A., and Douce, R. (1991) *Eur. J. Biochem.* **200**, 477–482.
23. Xia, J. H., and Saglio, P. H. (1992) *Plant Physiol.* **100**, 40–46.
24. Kanamori, K., Ross, B. D., and Tropp, J. (1995) *J. Magn. Reson. Ser. B* **107**, 107–115.